J Therm Anal Calorim (2012) 109:1169–1176
DOI 10.1007/s10973-012-2386-3

Effect of compositional gradient on thermal behavior of synthetic graphite–phenolic nanocomposites

Ehsan Bafekrpour · George P. Simon · Chunhui Yang · Jana Habsuda · Minoo Naebe · Bronwyn Fox

NATAS2011 Conference Special Chapter

Abstract Synthetic graphite–phenolic nanocomposites were designed and synthesized with a compositional gradient which is shown to influence transient temperature fields during rapid temperature changes. Such nanocomposites were fabricated using a compression moulding technique, and thermal conductivity and heat capacity of nanocomposites were experimentally determined using a modified transient plane source technique over a wide temperature range from 253.15 to 373.15 K. The effects of four compositional gradient configurations on the transient temperature field across the thickness of a nanocomposite plate, at a high imposed temperature, was investigated. The transient time and temperature fields in nanocomposite structures were highly affected by the compositional gradient configurations.

Keywords Synthetic graphite · Phenolic · Nanocomposites · Thermal conductivity · Heat capacity · Finite element modelling · Transient heat transfer

E. Bafekrpour (✉) · M. Naebe · B. Fox
Institute for Frontier Materials, Deakin University, Locked Bag 20000, Geelong, VIC 3220, Australia
e-mail: ebaf@deakin.edu.au

G. P. Simon · J. Habsuda
Department of Materials Engineering, Monash University, Clayton, VIC 3800, Australia

C. Yang
School of Engineering, Deakin University, Locked Bag 20000, Geelong, VIC 3220, Australia

Introduction

The superior properties of graphite have made it the material of choice for nanoscale reinforcement of polymer nanocomposites. Remarkable thermal [1–3], mechanical [4] and electrical [5] properties have been reported for graphite-reinforced polymers. These nanocomposites have potential structural applications in numerous fields, particularly in thermal environments such as those in aerospace applications where materials must withstand rapid temperature changes. The side of the structure exposed to the temperature change tends to expand or contract, while the other side resists, leading to thermal stresses in the structure. If the induced thermal stress reaches the yield strength of the material, then cracking or thermal shock occurs. One possible concept of decreasing the induced thermal stress is to decrease the transient time and temperature gradient within the structure [6]. Therefore, a transient thermal analysis is required to investigate the optimal composition in synthetic graphite (SG)–phenolic nanocomposites subjected to an in-plane heat flux.

Several numerical and analytical studies have been devoted to transient thermal analysis to investigate the effect of main parameters in composites. Zhou et al. [7] used a diffusion model to show that the graded parameter and the heat transfer parameter have a significant effect on the temperature distribution of a continuously graded ceramic/metal composite strip in contact with the well-stirred fluid. Cho et al. [8] studied the effects of the material variation through the thickness in functionally graded composites on temperature gradient and resulting thermal stress to optimize and control thermal stress using the finite element method. It has been reported that in-plane direction (not through the plate thickness direction) properties variation with a power law, considerably affects both

in-plane temperature distributions and heat-transfer periods in a ceramic/metal composite plate subjected to an in-plane heat flux [6] and edge heat flux [9].

In most studies in the literature to date, material and property gradients are considered continuous (linear, quadratic or exponential). However, discrete layer-by-layer material gradients are also produced in actual applications to optimize material properties. Agarwal et al. [10] obtained time-dependent temperature profiles in laminates having discrete layers of ceramic and metal composites. Effect of layer stacking sequence in laminated composites under dynamic conditions was examined by Tian et al. [11]. As the material deals with rapid temperature change in transient thermal analysis, temperature-dependent thermal properties must be used in the analysis to obtain more accurate results. However, temperature-independent properties have been used in most of the analyses performed in the literature. To the best of the authors' knowledge, no transient thermal analysis in nanocomposites, based on temperature-dependent properties of the constituents has been reported in the literature.

In this study, the effect of the compositional gradient configuration in SG–phenolic nanocomposite plates on transient temperature distribution is investigated. The plate consisted of eight layers and four composing nanocomposite materials including 0, 5, 10, and 20 wt% SG. Four stepwise compositional gradient configurations across the thickness were considered, by changing the sequence of the composing materials in layers. Firstly, thermal conductivity and heat capacity of the composing nanocomposites were experimentally determined over a wide temperature range from 253.15 to 373.15 K using modified transient plane source (MTPS) technique. Secondly, the measured thermal properties were used to define temperature-dependent properties of the nanocomposites in a finite element model developed by using a commercial FEA package—Abaqus for the transient thermal analysis. Temperature history and transient temperature distribution along the compositional graded thickness of the plate at a high imposed temperature were then examined.

Materials and measurement of thermal properties

A phenolic thermosetting resin with ~9 % hexamethylenetetramine obtained from Hexion Specialty Chemicals Pty Ltd was used as the matrix material. Synthetic graphite nano-platelets with an average thickness of 100 nm and diameters in the range of 1–3 μm were supplied by Asbury Graphite Mills, which are produced of the heat treatment of carbonaceous materials with 99 % purity. The SG nano-platelets were dried in a vacuum oven at 313.15 K for 24 h to reduce the moisture content. The powder mixtures of SG and phenolic resin with 5, 10 and 20 wt% SG contents were ball milled (8,000 M, Mixer/Mill, Maker, Spex, USA) for 1 h to ensure homogeneous dispersion of SG within the phenolic resin. Premixed composite powders were settled in a die of a hot press and heated to 403.15 K for 10 min, and then pressed at 453.15 K and 15 MPa for 10 min and finally cooled down to the room temperature. The thermal conductivity and heat capacity of the nanocomposites containing 0, 5, 10 and 20 wt% SG, as the composing materials of the functionally graded nanocomposites, were measured with the C-Therm Thermal Conductivity Analyser employing the MTPS technique. This method uses heat reflectance, similar to hot wire testing. The modification is that the heating element is supported on a backing, thus allowing a one-directional heat flow. Therefore, the temperature of the heating element versus the time function is used to calculate the thermal conductivity and thermal effusivity [12]. MTPS is an indirect measurement of heat capacity. Derivation of heat capacity can be obtained using the thermal effusivity, thermal conductivity and density. The heat capacity, density and thermal conductivity can be expressed using the following equation:

$$C_p = \frac{e^2}{k.\rho} \tag{1}$$

where C_p is the specific heat capacity (J g^{-1} K^{-1}), e is the thermal effusivity, k is the thermal conductivity (W m^{-1} K^{-1}) and ρ is the density (g m^{-3}). Thermal properties were measured at a temperature range from 253.15 to 373.15 K. The hot-pressed disc-shaped samples with a diameter of 30 mm and the same thickness were placed on the thermal sensors covering the measuring area completely. Glycol, water and glycerine were used as the contact agent between the sensors and smooth surfaces of the samples for temperature ranges of 253.15–278.15, 278.15–343.15, and 343.15–373.15 K, respectively. The temperature was controlled in a Tenney Junior thermal chamber. The measurements at each temperature were performed after 1 h to allow enough time for the samples to reach thermal equilibrium. Ten measurements were conducted at each temperature. The density of nanocomposite layers was measured using AccuPyc 1330 Pycnometer. 1–1.5 g of each nanocomposite was put in the cylindrical container, and purge fill pressure of helium gas was set to 136.5 kPa with equilibration rate of 0.034 kPa/min. Ten measurements were run for each nanocomposite. The distribution of SG within the phenolic matrix was investigated using a scanning electron microscope (SEM Supra 55VP).

Finite element modelling

In order to understand the influence of compositional change on temperature field in the SG–phenolic

nanocomposites plates, a finite element-based transient thermal analysis was developed and performed. The geometry and boundary conditions are shown in Fig. 1. To be able to assign the stepwise variation in material properties of the experimentally produced functionally graded SG–phenolic nanocomposites, a square plate with length of 300 mm and thickness of 5 mm, consisting of eight layers with the same thickness of 0.625 μm was developed by means of commercial finite element software, Abaqus [13].

Four compositional gradient configurations were considered, as illustrated in Table 1. To analyse transient heat conduction, the temperature-dependent thermal properties must be known which are measured experimentally in this study. In this model, the thermal properties of each layer for analysis vary according to the temperature of that layer at any time during analysis. Each layer was considered homogeneous, isotropic and having the thermal properties constant within the layer and different from the adjacent layer.

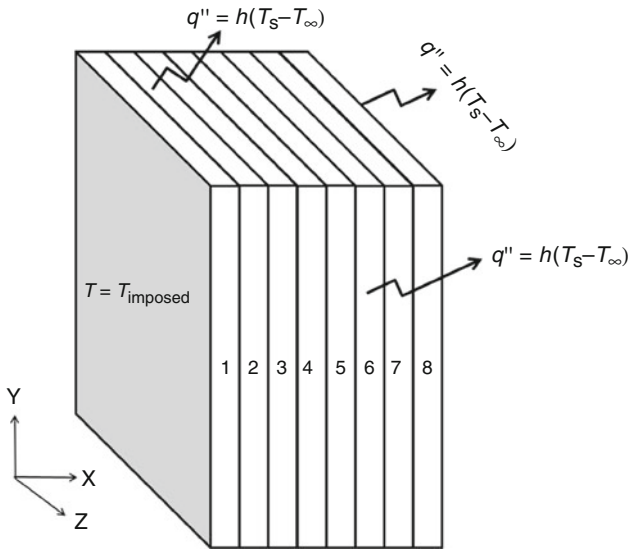

Fig. 1 Schematic diagram of layers and boundary conditions of the plate. The bottom and back side of the plate were assumed to have free convection heat transfer as well

Table 1 Variation of synthetic graphite weight fraction (wt%) in four compositional gradient configurations across the thickness of the plate

Configuration no.	Layer no.							
	1	2	3	4	5	6	7	8
1	20	10	5	0	0	5	10	20
2	0	5	10	20	20	10	5	0
3	0	0	5	5	10	10	20	20
4	20	20	10	10	5	5	0	0

The plate was assumed to initially be in thermal equilibrium with environment at room temperature, and subsequently, one side of the plate was suddenly exposed to the temperature of T. Free convection in air at 298.15 K was considered for the five rest sides of the plate with the convective heat transfer coefficient of $h = 10$ W m^{-2} K^{-1}. Perfect bonding between the layers was assumed. Mesh sensitivity and convergence of the model were checked by changing the number of linear hexahedral elements (1,728, 4,096, 8,000, 13,824 and 21,952). Based on this, the FE model was constructed from 13,824 elements of type DC3D8 and 17576 nodes as shown in Fig. 2. In doing so, 12 elements were used across the thickness (0.625 μm) of each layer. The temperature history and transient temperature distribution across the thickness of the plate were obtained for a imposed temperature of a high value ($T = 373.15$ K).

Results and discussion

The SEM micrographs of the cross sections of the phenolic and nanocomposites are shown in Fig. 3. The SGs were uniformly distributed within the matrix, even at a very high SG content (i.e. 20 wt%) and no agglomerated or clustered SG was observed.

Thermal conductivity of the materials composing the layers of the plate containing 0, 5, 10 and 20 wt% SG is shown in Fig. 4. It is seen that incorporating SG into the phenolic matrix increased the thermal conductivity of the resin. Depending on the SG content, the thermal conductivity enhancement varied from 33 % (nanocomposites with 5 wt% SG) to 140 % (nanocomposites with 20 wt% SG) at room temperature (298.15 K). The thermal conductivity of the nanocomposite containing 20 wt% graphite was considerably higher than that of other nanocomposites with less SG contents, most probably due to the formation of an interconnected network of SG

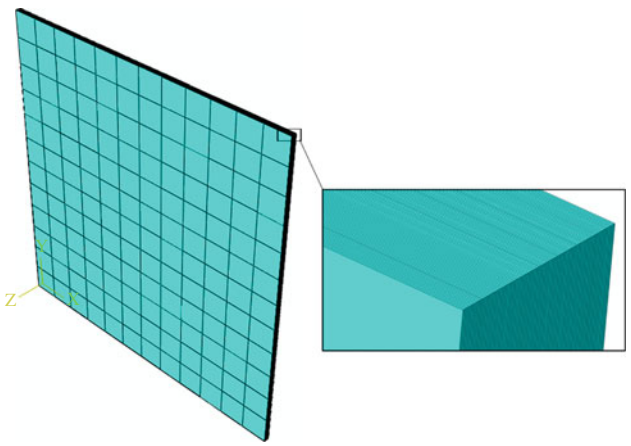

Fig. 2 3D finite element mesh for the square plate

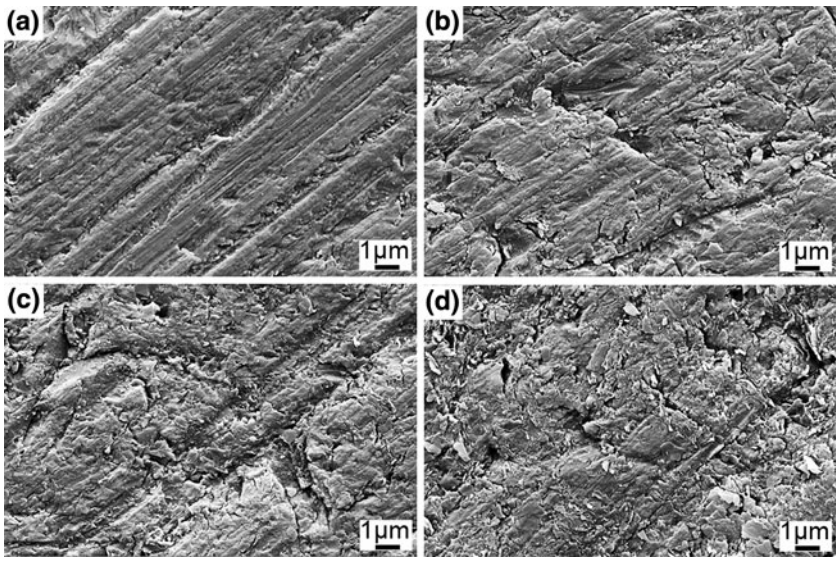

Fig. 3 SEM micrograph of the cross section of nanocomposites: **a** phenolic, **b** 5 wt% SG, **c** 10 wt% SG and **d** 20 wt% SG

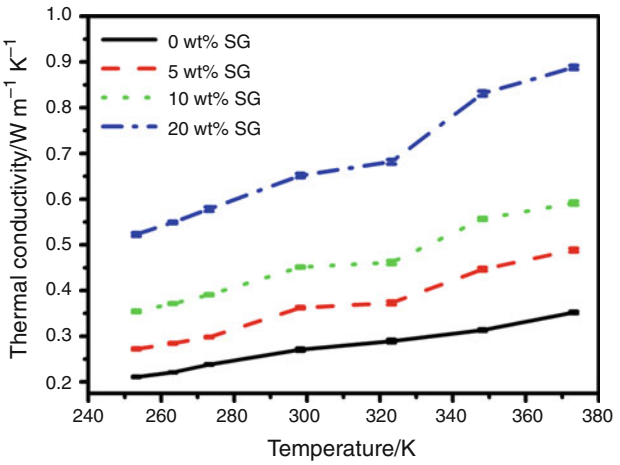

Fig. 4 Thermal conductivity of the nanocomposites containing 0, 5, 10 and 20 wt% synthetic graphite

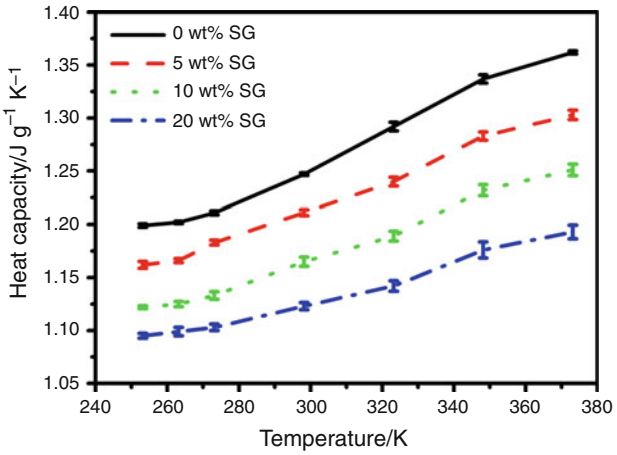

Fig. 5 Heat capacity of nanocomposites containing 0, 5, 10 and 20 wt% synthetic graphite

within the matrix. This improvement in thermal conductivity is in a good agreement with what has been reported for adding graphite to Nylon 66 [1] and epoxy [14] as well as multi-wall carbon nanotubes to epoxy composites [15]. Thermal conductivity of nanocomposites also increased continuously with temperature at a temperature range from 253.15 to 373.15 K. The small standard deviations of thermal conductivity of the samples indicate that the SG is uniformly distributed within the matrix.

The heat capacity of the SG–phenolic nanocomposites is shown in Fig. 5. It can be found that the heat capacity of the nanocomposites increased with increasing temperature. These results are consistent with the fact that the heat capacity of carbon nanotubes [16, 17], graphite [18, 19], and thermosetting matrix such as epoxy [20], increase with temperature rise. This phenomenon is due to higher level of molecular vibrations at elevated temperatures [21, 22]. The heat capacity of the nanocomposites decreased with the SG content. For example, the heat capacity of the phenolic matrix at room temperature decreased by 2.4, 6.4 and 9.6 % by adding 5, 10 and 20 wt% SG into the phenolic matrix. These results are consistent with reported decrease in the heat capacity of epoxy with graphite content [14].

The experimental measurements were then used to define the temperature-dependent thermal properties of the layers for the FEA-based transient heat-transfer analysis to investigate the influence of compositional configurations on temperature gradient field across the thickness. The densities of nanocomposites containing 0, 5, 10 20 wt% SG was 1.18, 1.29, 1.31 and 1.36 g cm^{-3}, respectively. Figure 6 shows transient temperature distribution across the thickness of the plate for four compositional gradient configurations at the imposed temperature of 373.15 K at different times.

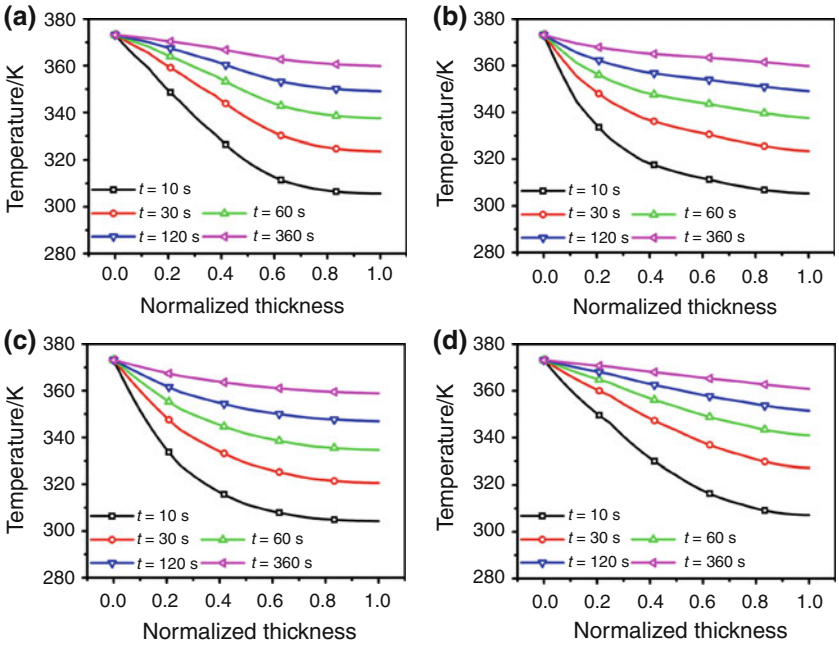

Fig. 6 Transient temperature distribution across the thickness for the imposed temperature of 373.15 K on the left side of the plate for **a** configuration-1, **b** configuration-2, **c** configuration-3 and **d** configuration-4

It can be seen that despite the same thickness and SG content in all four gradient configurations, configuration-4, with a decrease in thermal conductivity from the exposed side to the other, had the lowest temperature gradient field. It showed 3.56, 3.75 and 6.64 K lower temperature gradient between two sides of the plate after 30 s compared to thoes of configuration-1, -2 and -3, respectively. A low temperature gradient, especially in the very early stages of temperature exposure of the structure, has been reported to have significant effects on decreasing the induced thermal stresses and enhancing lifetime [6]. It can be also seen that the temperature gradient field decreases with time in all configurations. Configuration-1 showed a very similar temperature gradient field to configuration-2 at all the times, which indicates that the thermal properties of the surface layers contribute to temperature field, but that the properties of the other layers also affect the transient temperature distribution significantly. The plate with a gradual decrease in SG content from the exposed side has the lowest temperature gradient. Figure 7 shows temperature history of the layers of the plate for four compositional gradient configurations at the imposed temperature of 373.15 K.

It can be seen that the temperature of the layers suddenly increases at the early few seconds of the temperature exposure, which shows a transient temperature field across the thickness. After a while, the temperature change of layers with time is negligible which is indicative of steady-state heat transfer. The first stage is a critical one in term of thermal shock, as the induced thermal stress in this state is much higher than that of steady state [23]. It can be seen that configuration-4 reached its steady state the most rapidly amongst all configurations. Its transient time across the thickness was 46, 48 and 85 s shorter compared to configuration-1, -2, and -3, respectively. This decrease in transient time increases the possibility that the material will expand or contract more evenly. These results suggest that, transient time can be significantly reduced by controlling the microstructure across the thickness of the nanocomposites. The temperature gradients between the exposed side of the plate and the centre, as well as the exposed side and the opposite side after 30 s are reported in Table 2.

Configuration-4 was observed to have the lowest temperature gradient, followed by configuration-1, -2, and -3. Although the difference between configuration-4 and -1 was approximately of the same magnitude as thoes between configuration-1 and -3, configuration-1 and -2 interestingly showed very similar transient time and temperature gradient between the two sides of the plate. However, the difference in the temperature gradient of configuration-1 and -2 is more significant between the exposed side and centre. This could be due to variations in composition and corresponding thermal properties through the thickness of the plate. In order to investigate the effect of thermal conductivity (wt% SG) and the number of SG-containing layers on transient temperature distribution and temperature gradient across the thickness, we analysed a plate in which only the first layer contained SG (5, 10, and 20 wt%) and the remaining seven layers contained pure phenolic. Similarly, plates in which the first two, three and four layers contained SG were examined, and the results are presented in Fig. 8.

The temperature gradient between the two sides of the plate was highly affected by SG content and corresponding

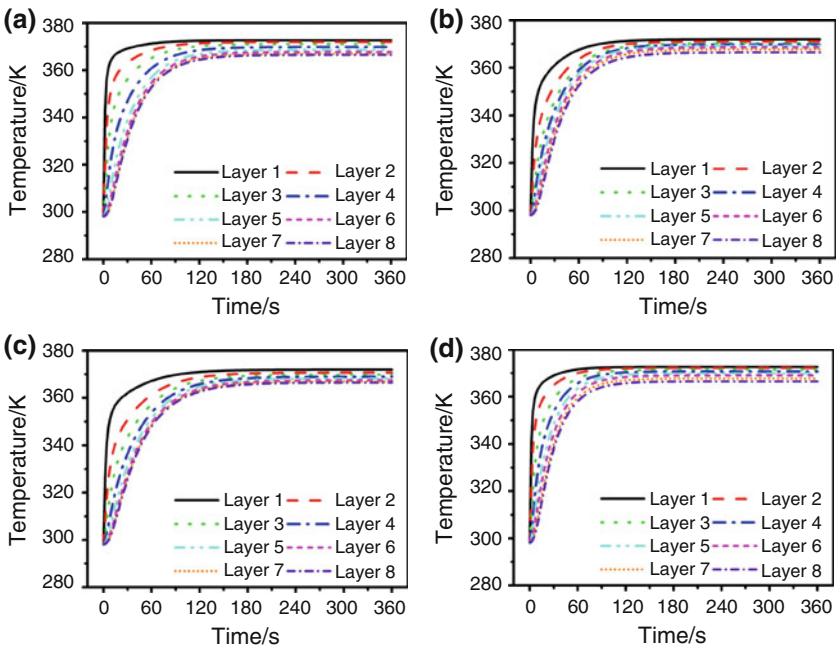

Fig. 7 Temperature history of each layer for the imposed temperature of 373.15 K on the left side of the plate for **a** configuration-1, **b** configuration-2, **c** configuration-3 and **d** configuration-4

Table 2 Temperature gradient after 30 s and transient time in four compositional gradient configurations

Configuration no.	Temperature gradient between the exposed and opposite sides/K	Temperature gradient between the exposed side and center/K	Transient time/s
1	49.53	35.54	210
2	49.72	39.50	212
3	52.61	44.02	249
4	45.97	30.00	164

variations in thermo physical properties, such as thermal conductivity, heat capacity and density. For example, in the case of a phenolic plate containing SG only in the first four layers, the temperature gradient decreased about 7, 12 and 20.3 % with 5, 10 and 20 wt% SG, respectively, compared with a pure phenolic plate. Also, the temperature gradient was influenced by the number of SG-containing layers. For instance, it decreased from 57.16 K in a pure phenolic plate to 54.36, 51.47, 48.51 and 45.54 K in a plate containing 20 wt% SG in layers No. 1, 1 and 2, 1–3 and 1–4, respectively. Similar effects of compositional gradient on

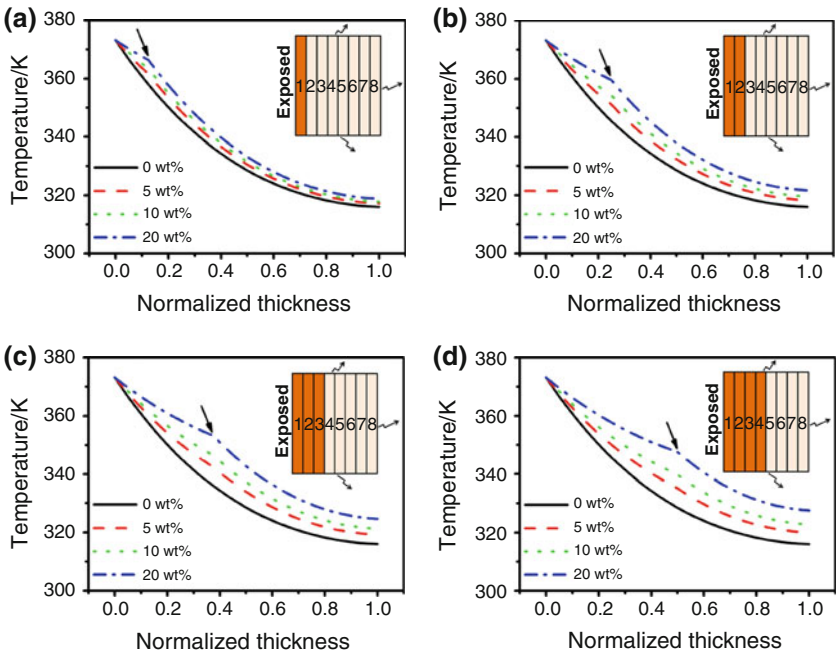

Fig. 8 Transient temperature distribution across the thickness for the imposed temperature of 373.15 K on the left side of the polymer plate with **a** layer no. 1 containing SG and layers no. 2–8 pure phenolic, **b** layers no. 1–2 containing SG and layers no. 3–8 pure phenolic, **c** layers no. 1–3 containing SG and layers no. 4–8 pure phenolic, and **d** layers no. 1–4 containing SG and layers no. 5–8 pure phenolic

transient thermal behaviours have been reported for continuously graded ceramic/metal composite strips [7]. Compared to configuration-4 (which was the best among all configurations, with a total SG content of 8.75 wt% and a temperature gradient of 45.97 K), only the plate containing 20 wt% SG in the first four layers had a slightly lower temperature gradient of 45.54. However, the latter had a higher total SG content (10 wt%) compared with configuration-4. Moreover, a smooth variation in the transient temperature distribution across the thickness of the plate with gradual compositional gradient was noted in Fig. 6 while a sharp variation is observed in Fig. 8, shown by arrows. This sudden variation is the result of mismatch in thermal properties through the thickness of the plate where SG-rich layers meet pure phenolic layers. Therefore, the plate with a gradual decrease in SG content had the optimized compositional gradient. The studied plate is heterogeneous as the composition and properties change across the thickness. However, each nanocomposite layer was assumed homogeneous and isotropic, and their overall bulk thermal properties were used for analysis. Therefore, the same results can be achieved for other materials with the same bulk properties. The results in terms of temperature distribution, transient time, and temperature gradient can be used for designing other composite materials with different properties. However, as the results are significantly dependent on thermal conductivity and heat capacity, analysis is required for the optimized composition.

Conclusions

We have demonstrated that transient temperature gradient field within the nanocomposites structures can be reduced by controlling the microstructure and composition. Transient temperature distribution and temperature history of four compositional gradient configurations in a SG–phenolic nanocomposite plate were analysed using a finite element method. The experimentally measured, temperature-dependent thermal properties were used in transient thermal analysis to improve the accuracy of the model. Transient time and temperature gradient field in SG nanocomposite structures are highly affected by the compositional gradient configuration. The results show that the nanocomposite plate with a gradual decrease in SG content from the exposed side to the other has the lowest temperature gradient and the shortest transient time amongst all the four compositional gradient configurations at both low and high imposed temperatures. These composition-optimized nanocomposites may be useful as structures with long life in thermal environments which experience rapid temperature changes and thermal shock.

Acknowledgements The authors would like to acknowledge the financial support of Advanced Manufacturing Cooperative Research Centre (AMCRC). Ehsan Bafekrpour also would like to express his thanks to Dr. Khashayar Khoshmanesh for his helpful discussions and guidance.

References

1. Fukushima H, Drzal L, Rook B, Rich M. Thermal conductivity of exfoliated graphite nanocomposites. J Therm Anal Calorim. 2006;85(1):235–8. doi:10.1007/s10973-005-7344-x.
2. Wang N, Zhang X, Zhu D, Gao J. The investigation of thermal conductivity and energy storage properties of graphite/paraffin composites. J Therm Anal Calorim. 2011:1–6. doi:10.1007/s10973-011-1467-z.
3. Sihn S, Ganguli S, Roy AK, Qu L, Dai L. Enhancement of through-thickness thermal conductivity in adhesively bonded joints using aligned carbon nanotubes. Compos Sci Technol. 2008;68(3–4):658–65.
4. Kalaitzidou K, Fukushima H, Drzal LT. Mechanical properties and morphological characterization of exfoliated graphite-polypropylene nanocomposites. Compos A Appl Sci Manuf. 2007;38(7):1675–82.
5. Biswas S, Fukushima H, Drzal LT. Mechanical and electrical property enhancement in exfoliated graphene nanoplatelet/liquid crystalline polymer nanocomposites. Compos A Appl Sci Manuf. 2011;42(4):371–5.
6. Bagci MD, Apalak MK. Thermal residual stresses in one-directional functionally graded plates subjected to in-plane heat flux. Numer Heat Transf A Appl. 2011;60(1):50–83.
7. Zhou YT, Lee KY, Yu DH. Transient heat conduction in a functionally graded strip in contact with well stirred fluid with an outside heat source. Int J Heat Mass Transf. 2011;54(25–26):5438–43.
8. Cho JR, Oden JT. Functionally graded material: a parametric study on thermal-stress characteristics using the Crank–Nicolson–Galerkin scheme. Comput Methods Appl Mech Eng. 2000;188(1–3):17–38.
9. Apalak MK, Bagci MD. Thermal residual stresses in adhesively bonded in-plane functionally graded clamped plates subjected to an edge heat flux. J Adhes Sci Technol. 2011;25(15):1861–908.
10. Agarwal B, Upadhyay PC, Banta L, Lyons D. Transient temperature distribution in composites with layers of functionally graded materials (FGMs). J Reinf Plast Compos. 2006;25(5):513–42.
11. Tian M, Zhu S, Chen Q, Pan N. Effects of layer stacking sequence on temperature response of multi-layer composite materials under dynamic conditions. Appl Therm Eng. 2012;33–34:219–26. doi:10.1016/j.applthermaleng.2011.09.039.
12. C-Therm Technologies Ltd. http://www.ctherm.com/products/tci_thermal_conductivity/. Accessed 08 2011.
13. Hibbitt D, Karlson B, Sorensen P. ABAQUS user's manual, version 6.9. Rhode Island: Hibbitt, Karlson, Sorensen Inc; 2009.
14. Ganguli S, Roy AK, Anderson DP. Improved thermal conductivity for chemically functionalized exfoliated graphite/epoxy composites. Carbon. 2008;46(5):806–17.
15. Kuo CH, Huang HM. Responses and thermal conductivity measurements of multi-wall carbon nanotube (MWNT)/epoxy composites. J Therm Anal Calorim. 2011;103(2):533–42.
16. Xu F, Sun L, Zhang J, Qi Y, Yang L, Ru H, et al. Thermal stability of carbon nanotubes. J Therm Anal Calorim. 2011;102(2):785–91. doi:10.1007/s10973-010-0793-x.
17. Silva G, Musumeci A, Gomes A, Liu J-W, Waclawik E, George G, et al. Characterization of commercial double-walled carbon

nanotube material: composition, structure, and heat capacity. J Mater Sci. 2009;44(13):3498–503. doi:10.1007/s10853-009-3468-x.
18. Tan Z-C, Zhang J-B, Shang-He M. A low-temperature automated adiabatic calorimeter heat capacities of high-purity graphite and polystyrene. J Therm Anal Calorim. 1999;55(1):283–9. doi:10.1023/a:1010177331806.
19. Hone J, Batlogg B, Benes Z, Johnson AT, Fischer JE. Quantized phonon spectrum of single-wall carbon nanotubes. Science. 2000;289(5485):1730–3.
20. McHugh J, Fideu P, Herrmann A, Stark W. Determination and review of specific heat capacity measurements during isothermal cure of an epoxy using TM-DSC and standard DSC techniques. Polym Test. 2010;29(6):759–65.
21. Cecen V, Tavman IH, Kok M, Aydogdu Y. Epoxy- and polyester-based composites reinforced with glass, carbon and aramid fabrics: measurement of heat capacity and thermal conductivity of composites by differential scanning calorimetry. Polym Compos. 2009;30(9):1299–311.
22. Abbassi A, Khoshmanesh K. Numerical simulation and experimental analysis of an industrial glass melting furnace. Appl Therm Eng. 2008;28(5–6):450–9. doi:10.1016/j.applthermaleng.2007.05.011.
23. Peng X-L, Li X-F. Transient response of temperature and thermal stresses in a functionally graded hollow cylinder. J Therm Stresses. 2010;33(5):485–500.